DOI:
10.1016/j.jms.2017.03.007

Document Version
Peer reviewed version

Ethanol dimer: observation of three new conformers by broadband rotational spectroscopy

D. Loru, I. Peña, M. E. Sanz*

Department of Chemistry, King's College London, London SE1 1DB, United Kingdom

Abstract

The conformational behavior of the hydrogen-bonded cluster ethanol dimer has been reinvestigated by chirped pulse Fourier transform microwave spectroscopy in the 2-8 GHz frequency region. Three new conformers (*tt*, *tg*+, and *g*–*g*+) have been identified together with the three (*g*+*g*+, *g*–*t*, and *g*+*t*) previously observed by Hearn et al. (*J. Chem. Phys.* 123, 134324, 2005) and their rotational and centrifugal distortion constants have been determined. By using different carrier gases in the supersonic expansion, the relative abundances of the observed conformers have been estimated. The monosubstituted ^{13}C species and some of the ^{18}O species of the most abundant conformers *g*+*g*+, *g*–*t*, and *tt* have been observed in their natural abundance, which led to the partial determination of their r_s structures, and the r_0 structure for the *tt* conformer. The six observed conformers are stabilized by the delicate interplay of primary O–H···O and secondary C–H···O hydrogen bonds, and dispersion interactions between the methyl groups. Density functional and ab initio methods with different basis sets are benchmarked against the experimental data.

Keywords: alcohol, rotational spectroscopy, conformational analysis, non-covalent interactions, abundance

* Corresponding author. E-mail address: maria.sanz@kcl.ac.uk

1. Introduction

Non-covalent intermolecular interactions such as hydrogen bonding, London dispersion interactions and short-range steric repulsion play a major role in describing macroscopic properties of condensed phases, biological and synthetic materials, and pathways of catalytic reactions. The study of small clusters has thus aimed to determine the interaction sites and relative arrangement of the monomers, and identify the intermolecular forces at play. Understanding the properties of small clusters lays the ground for investigating larger and more complex systems. In particular, hydrogen-bonded clusters, especially those involving water, have received a lot of attention due to their crucial role in chemistry and biology[1,2]. Not as many studies have been devoted to alcohol-containing clusters, even if they are also relevant to elucidate solvation phenomena.

Ethanol dimer is an archetypal system for the investigation of the properties of hydrogen-bonded clusters where different types of interactions can take place, and specifically to understand the way in which the establishment of intermolecular hydrogen bonds affects the conformational preferences of the monomers. Bare ethanol is a flexible molecule that exists in a *trans* (*t*, with a CCOH dihedral angle of 180°) and in two enantiomeric *gauche* configurations (*g*+ and *g*–, with CCOH dihedral angles of +60° and –60°, respectively, see Fig. 1). The *trans* conformer is lower in energy by approximately 0.5 kJ mol^{-1} [3] and it is separated by the *gauche* configurations by barriers of *ca*. 400 cm^{-1} [4]. Therefore all three conformers coexist at room temperature, with the *gauche* configuration statistically favored by a factor of 2. The two equivalent *gauche* conformations interconvert through quantum tunneling[3] and so they are considered to be transient chiral molecules.

Formation of the ethanol dimer changes the conformational landscape described above. The two ethanol monomers interact through hydrogen bonding, which effectively prevents tunneling of the *gauche* conformations and makes it possible to distinguish dimers involving *g*+ and *g*– ethanol configurations, in an example of induced chirality. Depending on the configuration of the ethanol monomers, ethanol dimers can be classified into different families, corresponding to *tt*, *tg*+, *tg*–, *g*+*t*, *g*–*t*, *g*+*g*+, *g*+*g*–, *g*–*g*+ and *g*–*g*–, where the first letter designates the hydrogen bond donor and the second letter the acceptor. In addition, the proton donor molecule can interact with either lone pair of the acceptor oxygen, which are located on the right and on the left side of the OH bond (see Fig. 1). For each structure a mirror image is obtained by exchanging the lone pair involved in the hydrogen bond and the chirality of the gauche forms (g+/g-) in the dimer.

There have been several theoretical and experimental investigations of ethanol dimer[5-16]. Initial vibrational studies using molecular beam depletion[5], FTIR[6] and cavity ring-down spectroscopy[7] provided evidence for up to four conformations, although it was not possible to assign spectral features to individual conformers. Conformational identification was achieved by Hearn et al.[8], who observed three conformers of ethanol dimer and assigned them as the *g*+*g*+, *g*+*t*, and *g*–*t* (following the nomenclature above) using high resolution Fourier transform microwave spectroscopy. In addition, various theoretical calculations[7,8,9,10,11,12] have shown the complexity of the potential energy surface of the dimer, where a subtle interplay of hydrogen bonds (classical O–H···O and weak C–H···O) and dispersion interactions results in very small energy differences between the many lower-energy conformations and makes it difficult to predict molecular properties accurately. One of the persistent questions in the study of ethanol dimer was the identity of the lowest energy form. Theoretical calculations originally

predicted it to correspond to the *tt* species[9], but later calculations agreed on the homochiral *g*+*g*+ configuration as the global minimum[10,11,12]. This makes ethanol dimer an interesting example of chirality synchronization[13], where two transiently chiral ethanol molecules adjust to each other's handedness. Experimentally, the use of different carrier gases in supersonic expansions modifies the degree of relaxation of higher energy conformers to lower energy ones[14], with light He being the least efficient relaxant. Therefore, by changing the carrier gas it is possible to determine the identity of the global minimum and energy ordering of the different conformations. This effect has been explored in two different experiments in supersonic jets using FTIR[12] and Raman spectroscopy[15], where the vibrational band corresponding to the most stable species of ethanol dimer was assigned, and later in a recent microwave experiment which confirmed the *g*+*g*+ species as the global minimum[16].

In this work, we have reinvestigated the rotational spectrum of the ethanol dimer using broadband rotational spectroscopy[17], which can sample swiftly the contributions of different conformers coexisting in a sample since large sections of the spectrum are collected at once. Our work was prompted by observations of ethanol dimers that differed from those reported by a previous microwave study[8] while investigating complexes of ethanol with fenchone[18]. We have characterized six conformations of the ethanol dimer, three new conformations in addition to the three already identified[8]. The use of different carrier gases in the supersonic expansion to vary the extent of collisional relaxation has allowed us to establish the energy ordering of the conformations, confirming previous observations of the global minimum as the *g*+*g*+ species. Detection of several isotopically monosubstituted ^{13}C and ^{18}O species for the three most abundant conformers allows a first estimation of their substitution and effective structures. Theoretical calculations using density functional and ab initio methods have

also been performed to predict molecular properties and benchmark their performance against experimental data. The observed six conformations correspond to those theoretically predicted to be lowest in energy and with the largest binding energies at the highest level of theory used. The observations are rationalized in terms of the hydrogen bonds involved in the stabilization of the different conformers.

2. Methods

2.1. Experimental

The jet cooled rotational spectrum of ethanol dimer was recorded in the 2 to 8 GHz frequency range using our chirped-pulse Fourier transform microwave spectrometer (CP-FTMW) at King's College London, described elsewhere[19]. A chirped-pulse is directly generated by an arbitrary waveform generator and amplified by an adjustable travelling wave tube amplifier with 200 W maximum output power. Following amplification, two standard horn antennas separated approximately 40 cm are used to broadcast the excitation pulse into the vacuum chamber and receive the broadband molecular emission. This molecular free induction decay (FID) signal is directly digitized using a digital oscilloscope after amplification by a low-noise microwave amplifier. The detection branch of the electronics is protected from accidental damage by a pin diode and a microwave switch positioned in front of the low noise amplifier. All frequency and trigger sources as well as the digital oscilloscope are phase-locked to a 10 MHz Rb-disciplined quartz oscillator.

A commercial sample of ethanol (Fisher Scientific, >99%) was used without any further purification to generate ethanol dimer in the expansion. Ethanol, a liquid at room temperature, was placed in a heating reservoir attached to the nozzle and heated gently (at 303.15 K) to increase its concentration in the gas phase. Three different carrier

gases, He, Ne and Ar at constant backing pressures of 2 bar were used to seed vaporised ethanol into the vacuum chamber and obtain the three spectra of Fig. 2. Experimental conditions were optimised for each carrier gas to obtain the maximum intensity of the signal. Molecular pulses of 400 μs, 1100 μs and 600 μs were used for He, Ne and Ar, respectively, to produce the supersonic jet. Microwave chirped pulses of 4 μs were applied with a delay of 600 μs, 1200 μs and 800 μs with respect to the start of molecular pulse, for He, Ne and Ar, respectively. Taking advantage of the "multi-FID" operation mode to reduce the measurement time and sample consumption,[17] four FIDs were acquired on each injection cycle, separated by 30 μs. Each FID was detected for 20 μs. The frequency domain spectra were obtained by taking a fast Fourier transformation at a 4 Hz repetition rate, following the application of a Kaiser-Bessel window to improve baseline resolution. Line widths of approximately 110 kHz full-width-half-maximum (FWHM) are achieved.

2.2. Theoretical

Building on previous theoretical calculations of ethanol dimer[8,12], the local minima of ethanol dimers have been optimized at MP2 and M062X levels with the standard basis sets 6-311++G(d,p) and 6-311++G(3df,2p) using Gaussian 09 package[20]. Of the two mirror images resulting from having the right or left lone pair of oxygen involved in hydrogen bonding, we will refer only to those structures where the right lone pair participates in hydrogen bonding as their rotational spectra are indistinguishable from those involving the left lone pair. The different conformers have been labelled following the nomenclature of ref. [12]. The calculations provide the relative energy of conformers, the rotational constants (*A, B, C*) and electric dipole moment components (μ_a, μ_b, μ_c) relevant for our rotational studies (see Table 1 and Tables S1-S4 in the Supplementary Information). Harmonic frequency calculations at

the corresponding levels of theory were performed to confirm that all optimized geometries were local minima and to calculate their zero-point energies. The dissociation energies of the complexes have also been calculated, including corrections for the basis set superposition error using the counterpoise procedure[21] and fragment relaxation terms[22].

3. RESULTS AND DISCUSSION

3.1. Rotational spectrum

The broadband rotational spectrum of ethanol dimer in the 2-8 GHz frequency range was first recorded using Helium as carrier gas (see Fig. 2). The rotational transitions corresponding to the three conformers of ethanol dimer characterized in a previous microwave spectroscopic study[8], *g*+*g*+, *g*+*t* and *g*–*t*, (corresponding to G2G, T1G, and T2G, respectively, in the nomenclature of ref. [8]) were readily identified. A total of 23, 31 and 17 rotational transitions were measured for the *g*+*g*+, *g*–*t*, and *g*+*t* configurations, respectively (see Tables S5-S7 of the Supplementary Information), and were fit using the Watson Hamiltonian in the S reduction and I^r representation[23] and Pickett's program[24] to yield the set of the experimental rotational and quartic centrifugal distortion constants in Table 2. Our determined parameters are in excellent agreement with those of ref. [8]. Our rotational constants are better determined, but the lower *J* values only allow determination of three centrifugal distortion constants. Therefore we included the rotational transitions of ref. [8] in our fit, giving them an uncertainty of 2 kHz, and an uncertainty of 10 kHz to the lines measured in this work by CP-FTMW spectroscopy (see Tables S8-S10 for residuals). The improved rotational and centrifugal distortion constants are displayed in Table 2.

After removing the lines assigned to the three conformers above, there was still a significant number of lines in the rotational spectrum. There are other conformations of ethanol dimer predicted by theory to have energies close to the already identified conformers *g*+*g*+, *g*+*t* and *g*–*t*, and with sizable dipole moment components along the principal inertial axes (see Table 3). Since they all have large μ_a dipole moment components, their *a*-type transitions of the series $J + 1 \leftarrow J$ were first searched for. Three separate sets of transitions corresponding to three different species were initially identified, and assignments were further confirmed with the prediction and measurement of additional transitions (see Tables S11-S13). The final rotational and centrifugal distortion constants, determined by fitting transitions to the same Hamiltonian as above, are shown in Table 3. Conformational identification of the new species can be achieved by comparing the experimental and theoretical values of the molecular properties (Tables 1 and 3). Experimental values of the rotational constants of the three new conformers I, II, and III nicely match with those predicted by *ab initio* calculations for conformers *tt*, *g*–*g*+ and *tg*+, respectively.

Conformational assignment of all species is supported by the consistency between the type of transitions detected and the predicted values of μ_a, μ_b and μ_c, since different arrangements of the two ethanol molecules produce drastic changes in the values of the *b*- and *c*-type dipole moment components. Hence the detection of *a*- and *c*-type transitions in rotamer I is consistent with the near-zero value of μ_b predicted for conformer *tt*. Similarly, only *a*- and *c*-type transitions have been observed for conformer *g*+*t*. Theoretical values of μ_a, μ_b and μ_c for conformers *g*–*t* and *g*+*g*+ are also consistent with observations. For conformers *g*–*g*+ and *tg*+, *b*- and *c*-type transitions were not detected; however, this is to be expected considering the intensity of their *a*-type transitions and the lower predicted values of μ_b and μ_c.

From the comparison between experimental and theoretical rotational constants at the various levels (see Table 1 and Tables S1-S4), MP2 performed better than M062X. Interestingly, the 6-311++G(d,p) basis sets provided constants with less percentage errors than 6-311++G(3df,2p). The percentage errors varied across the different conformations, with conformers having *trans* ethanol as the hydrogen acceptor showing the largest deviations, of up to 4.0% and 4.8% for the *B* and *C* rotational constants of conformer *g*+*t*, while the largest deviation for dimers with *gauche* ethanol as hydrogen bond acceptor was 1.6% for the *A* rotational constant of *tg*+ and the *B* rotational constant of *g*+*g*+.

3.2. Conformational energy ordering

Further experiments with Ne and Ar as carrier gases were conducted to estimate an energy ordering of the conformers. The rotational spectrum recorded using Ne as carrier gas (Figure 2, middle) showed a much better signal-to-noise ratio than the one with He but only three conformers, *g*+*g*+, *g*–*t*, and *tt*, could be detected. In the Ar jet spectrum only one conformer, homochiral *g*+*g*+, was present (Figure 2, bottom), confirming that is the lowest energy form in agreement with results reported by Finneran et al.[16] Considering the results above, the conformers *g*–*t* and *tt* detected in a Ne expansion are the next conformers in energy ordering above the global minimum, and the three conformers detected only in He, the higher energy ones. In addition to these observations, we have carried out careful relative intensity measurements of the measured *a*-type transitions common to all conformations, and corrected them considering that transition intensity is proportional to the square of the corresponding dipole moment component μ_a. The relative abundances of the ethanol dimer conformers in He follow the order *g*+*g*+ > *g*–*t* ≈ *tt* > *g*+*t* ≈ *tg*+ > *g*–*g*+.

The detected conformers are those predicted to have the largest binding energies at the highest level of theory used, MP2/6-311++G(3df,2p). MP2 calculations with the two different basis sets used in this work correctly predict the six observed conformers as the lowest in energy, with and without zero-point corrections. However, the predicted energy ordering is not consistent with observations for any of the methods used, although it should be pointed out that the differences are very small and within the accuracy of the calculations (see Table 1 and Tables S1-S4).

3.3. Isotopic Species and Structural Determination

The large signal-to-noise ratio of the rotational spectrum recorded with Ne as a carrier gas allowed the observation of the monosubstituted ^{13}C isotopic species of the *g+g+*, *g–t*, and *tt* conformers in their natural abundance of 1.1%, and the monosubstituted ^{18}O isotopologues (0.2 % abundance) for the *tt* conformer (see Fig. 3 for numbering of the heavy atoms). Predicted frequency shifts for these species were consistent with those observed experimentally, further supporting identification of these conformers. All measured transitions for the isotopologues (see Tables S14−S27 of the Supporting Information) were fit with the same Hamiltonian as the parent conformers and keeping the values of the centrifugal distortion constants fixed to those determined for the parent conformers. The experimental rotational constants are displayed in Tables 4-6.

The substitution coordinates of the most abundant conformers of ethanol dimer were derived from the isotopic information according to the Kraitchmann method[25] and using the program KRA[26]. Some of the carbon atoms are very close to the principal inertial axes, which led to imaginary values of their substitution coordinates in some cases. Imaginary coordinates were set to zero for the determination of structural

parameters. The large uncertainties in the values of the *A* rotational constants for the isotopic species, due to the reduced line set, led to substantial errors in some of the coordinates (see Tables 7-9). Nevertheless, in general there is a good agreement between the experimental and theoretical values of the coordinates.

Partial substitution structures r_s were determined from the experimental coordinates of Tables 7-9 using the program EVAL[26] (see Tables 10-12). All coordinates, including those set to zero, carried Costain's error[27] to include vibration-rotation effects. For the *tt* conformer, five distances, three angles and two dihedral angles involving all heavy atoms were determined, while for the *g*+*g*+ and *g*–*t* conformers only the two distances and one dihedral angle involving the carbon atoms could be determined. Additionally, the effective structure r_0 of the *tt* conformer was determined through least-squares fit of the experimental moments of inertia of the observed isotopologues using the STRFIT program[26] (see Table 10). The structural parameters that were not floated in the fit were kept fixed to the MP2/6-311++G(d,p) theoretical values, as this level of theory yielded the rotational constants closer to the experimental ones. Attempts to determine r_0 structural parameters for the *g*+*g*+ and *g*–*t* conformers, floating different combinations of distances and angles, resulted in non-convergent fits.

The structural parameters obtained are compared with those from theoretical calculations in Tables 10-12. For the *tt* conformer, there is a reasonable agreement between the different structures, but there are also some striking differences. The torsional angle $\angle C_2–O_3–O_4–C_5$, which reports on the relative orientation of the two ethanol monomers, differs by about 15% between the r_s and r_0 structures, although both values carry large errors. Similar variations can be observed for the other dihedral angles reported. These changes are mirrored by the variation in the values predicted by

MP2 and M062X methods. There is also a significant discrepancy in the values of $\angle O_3–C_2–C_1$, which also have substantial uncertainties. In this case the r_s value is closer to the theoretical values, which are in close agreement. The experimental substitution and effective distances involving the oxygen atoms also show notable variations: the r_0 distance $r(O_3–C_2)$ is ~4% lower than the r_s and theoretical values, and the r_0 value of distance $r(O_4–C_5)$ about 9% higher than the r_s and theoretical values. For the *g*+*g*+ and *g*–*t* conformers (see Tables 11 and 12) the r_s parameters carry large uncertainties, reflecting the uncertainties in the |*a*|, |*b*|, and |*c*| coordinates.

All the above underlies the challenges in determining the structure of a floppy complex such as ethanol dimer. A more accurate r_s structure of ethanol dimer can probably be achieved by improving the determination of the rotational constant *A*. Use of different methods and basis sets to more accurately describe the experimental complex will improve the determination of the r_0 structural parameters, since some of them will have to remain fixed to theoretical values. In summary, the data provided here can be taken as a good starting point for an improved description of the structure of this prototypical hydrogen-bonded complex.

3.4. Conformational Preferences and Interactions

The observed relative abundances of the ethanol dimer conformer, *g*+*g*+ > *g*–*t* ≈ *tt* > *g*+*t* ≈ *tg*+ > *g*–*g*+, stem from a subtle balance of intermolecular forces, involving hydrogen bonds and, in some cases, dispersion interactions. All conformers exhibit a primary O–H···O hydrogen bond linking the two hydroxyl groups, with predicted distances 1.89-1.91 Å at the MP2/6-311++G(d,p) level of theory, which provides the closest agreement with experimental rotational constants (see Fig. 4). In addition, all conformers show weak C–H···O interactions between the methyl group of the hydrogen

acceptor ethanol monomer and the oxygen in the donor ethanol, with distances in the range between 2.79 – 2.92 Å. The conformers *g*+*g*+, *g*–*t*, *g*+*t* and *g*–*g* (all except those with a *trans* ethanol as hydrogen bond donor) also show weak C–H···O interactions between the $–CH_3$ of the donor ethanol and the oxygen of the acceptor ethanol, with distances of 2.9-3.0 Å except for the *g*–*g*+ conformer that shows a distance of 3.2 Å. All conformers present dispersion interactions between the $–CH_3$ and $–CH_2$ groups of the ethanol monomers except *tg*+ and *g*–*g*+, which are two of the higher energy conformers observed. The other higher-energy dimer *g*+*t* is predicted to have the longest hydrogen bond. To summarise, the observed energy ordering can be rationalised in terms of all these various interactions, with the lower energy forms showing shorter (stronger) hydrogen bonds and dispersion interactions, and the higher energy forms presenting no dispersion interactions and longer C–H···O interactions.

The homochiral form *g*+*g*+, an example of chirality synchronization[13], is clearly preferred over the heterochiral form *g*–*g*+ in ethanol dimer, which is the least abundant form, less abundant than forms involving mixed trans-gauche ethanol conformers. Interestingly, the related 2,2,2-trifluoroethanol (TFE) dimer[28] also displays a strong preference for the homochiral form. However, this preference is not maintained in other related dimers such as 2-fluoroethanol (2FE),[29] where the heterochiral conformer is slightly favored. Heterochiral forms are also preferred in larger alcohols such as 2-propanol[30] and 2-butanol[31]. All the above dimers present several coexisting conformers within a small energy range, and thus it is expected that a preference for either the homo or heterchiral forms arises from slight changes in the balance of intermolecular forces.

The switch from *trans* to *gauche* ethanol upon complexation has also been observed for the ethanol-water complex[32,33,34,35]. However, this is not a widespread occurrence. In the ethanol-methanol complex[16] ethanol remains in the *trans*

configuration in the lowest energy conformation, and in complexes of ethanol with other partners (including NH_3[36], dimethylether[37], and oxirane derivatives[38,39]) both *gauch*e and *trans* ethanol have been found to participate in the lowest-energy form. All ethanol complexes above show several configurations very close in energy, which arise from the ease of ethanol to switch conformations and therefore makes it difficult to predict which conformation will be adopted by ethanol in the global minimum. In the related alcohols 2FE[40] and TFE[41], gauche conformers are strongly favored, which results in lower-energy dimers involving only gauche conformers[28,29].

The number of observed low-energy conformers increases in the series of complexes of ethanol with water (HO–H), methanol (HO–CH_3) and ethanol (HO–CH_2CH_3), due to the existence of a longer alcohol chain and the additional weak interactions that can be established. In this respect, it will be interesting to study mixed dimers of ethanol with longer alcohols to find out whether this trend is maintained.

5. Conclusions

The interesting problem of conformational isomerism in ethanol dimer has been reinvestigated using CP-FTMW spectroscopy. Three new conformers (*tt*, *tg*+, and *g*–*g*+) have been identified together with the three (*g*+*g*+, *g*–*t*, and *g*+*t*) previously characterized by microwave spectroscopy[8], and their rotational and centrifugal distortion constants have been determined. Several isotopologues in natural abundance have been observed for the three most abundant conformers *g*+*g*+, *g*–*t*, and *tt*, which led to the partial determination of their substitution structures, and an effective structure for the *tt* conformer.

The use of different carrier gases in the supersonic expansion to tune conformational relaxation has made it possible to establish the energy ordering of the

six observed conformers, confirming the homochiral conformer *g+g+* as the lowest energy form of ethanol dimer. A fine balance of several intermolecular interactions, involving classical O–H···O hydrogen bonds and weak C–H···O and dispersion interactions, determine the relative stability of the observed conformations. Overall, our results are a stepping stone for studies of larger aggregates of ethanol and can contribute to advance our understanding of the behavior of ethanol in the condensed phases.

Acknowledgements

This work was supported by the EU FP7 (Marie Curie Grant No. PCIG12-GA-2012-334525) and King's College London.

References

[1] S. N. Vinogradov, R. H. Linnell, *Hydrogen Bonding*, van Nostrand Reinhold Company, New York, 1971.
[2] G. A. Jeffrey, *An introduction to Hydrogen Bonding*, Oxford University Press, Oxford, 1997.
[3] J.C. Pearson, K.V.L.N. Sastry, E. Herbst, F.C. De Lucia, *J. Mol. Spectrosc*. 175 (1996) 246.
[4] R. K. Kakar, C. R. Quade, *J. Chem. Phys.* 72 (1980) 4300-4307.
[5] M. Ehbrecht, F. Huisken, *J. Phys. Chem. A* 101 (1997) 7768-7777.
[6] T. Häber, U. Schmitt, M. A. Suhm, *Phys. Chem. Chem. Phys.* 1 (1999) 5573–5582.
[7] R. A. Provencal, R. N. Casaes, K. Roth, J. B. Paul, C. N. Chapo, R. J. Saykally, G. S. Tschumper, H. F. Schaefer, III. *J. Phys. Chem. A* 104, (2000), 1423–1429.
[8] J. P. I. Hearn, R. V. Cobley, B. J. Howard, *J. Chem. Phys*. 123 (2005) 134324.
[9] L. González, O. Mó, M. Yáñez, *J. Chem. Phys.* 111 (1999) 3855.
[10] V. Dycmons, *J. Phys. Chem. A*, 108 (2004) 2080-2086.
[11] A. Vargas-Caamal, F. Ortiz-Chi, D. Moreno, A. Restrepo, G. Merino, J. L. Cabellos, *Theor. Chem. Acc.*, 134 (2015) 16.
[12] C. Emmeluth, V. Dyczmons, T. Kinzel, P. Botschwina, M. A. Suhm, M. Yáñez, *Phys. Chem. Chem. Phys.*, 7 (2005), 991-997.
[13] A. Zehnacker, M. A. Suhm, *Angew. Chem. Int. Ed*, 47 (2008) 6970-6992.
[14] R. S. Ruoff, T. D. Klots, T. Emilsson, H. S. Gutowsky, *J. Chem. Phys.*, 93 (1990) 3142-3150
[15] T. N. Wassermann, M. A. Suhm, *J. Phys. Chem. A*, 114 (2010) 8223-8233.
[16] I. A. Finneran, P. B. Carroll, G. J. Mead, G. A. Blake, *Phys. Chem. Chem. Phys*. 18 (2016) 22565–22572.
[17] G.G. Brown, B.C. Dian, K.O. Douglass, S.M. Geyer, S.T. Shipman, B.H. Pate, *Rev. Sci. Inst*rum. 79 (2008) 053103.
[18] D Loru, M. E. Sanz, *71st International Symposium on Molecular Spectroscopy*, Urbana-Champaign,(IL, USA), 19-26 June 2016, Talk WC11, Structural characterisation of fenchone and its complexes with ethanol by broadband rotational spectroscopy.
[19] D. Loru, M. A. Bermúdez, M. E. Sanz, *J. Chem. Phys*. 145 (2016) 074311.

[20] M. J. Frisch, G. W. Trucks, H. B. Schlegel, G. E. Scuseria, M. A. Robb, J. R. Cheeseman, G. Scalmani, V. Barone, B. Mennucci, G. A. Petersson, H. Nakatsuji, M. Caricato, X. Li, H. P. Hratchian, A. F. Izmaylov, J. Bloino, G. Zheng, J. L. Sonnenberg, M. Hada, M. Ehara, K. Toyota, R. Fukuda, J. Hasegawa, M. Ishida, T. Nakajima, Y. Honda, O. Kitao, H. Nakai, T. Vreven, J. A. Montgomery, Jr., J. E. Peralta, F. Ogliaro, M. Bearpark, J. J. Heyd, E. Brothers, K. N. Kudin, V. N. Staroverov, R. Kobayashi, J. Normand, K. Raghavachari, A. Rendell, J. C. Burant, S. S. Iyengar, J. Tomasi, M. Cossi, N. Rega, J. M. Millam, M. Klene, J. E. Knox, J. B. Cross, V. Bakken, C. Adamo, J. Jaramillo, R. Gomperts, R. E. Stratmann, O. Yazyev, A. J. Austin, R. Cammi, C. Pomelli, J. W. Ochterski, R. L. Martin, K. Morokuma, V. G. Zakrzewski, G. A. Voth, P. Salvador, J. J. Dannenberg, S. Dapprich, A. D. Daniels, Ö. Farkas, J. B. Foresman, J. V. Ortiz, J. Cioslowski and D. J. Fox, Gaussian 09, Revision E.01, Gaussian, Inc., Wallingford CT, 2010

[21] S. F. Boys, F. Bernardi, *Mol. Phys*. 19 (1970) 553-566.

[22] S. S. Xantheas, *J. Chem. Phys*. 104 (1996) 8821-8824.

[23] J. K. G. Watson, *Vibrational Spectra and Structure*, Elsevier, New York/Amsterdam, 1977

[24] H. M. Pickett, *J. Chem. Phys.*, 56 (1972) 1715.

[25] J. Kraitchman, *Am. J. Phys*. 21 (1953) 17.

[26] Z. Kisiel, *PROSPE - Programs for ROtational SPEctroscopy*, http://info.ifpan.edu.pl/˜kisiel/prospe.htm (accessed 14 Jan 2017).

[27] C. C. Costain, *Trans. Am. Crystallogr. Assoc*. 2, 157 (1966).

[28] J. Thomas, Y. Xu, *J. Phys. Chem. Lett.*, 5 (2014) 1850−1855.

[29] X. Liu, N. Borho, Y. Xu, *Chem. Eur. J.*, 15 (2009) 270-277.

[30] M. A. Snow, B. J. Howard, L. Evangelisti, W. Caminati, *J. Phys. Chem. A*, 115 (2011) 47-51.

[31] A. K. King, B. J. Howard, *Chem. Phys. Lett*, 348 (2001) 343-349.

[32] M. Nedic´, T. N. Wassermann, Z. Xue, P. Zielke, M. A. Suhm, *Phys. Chem. Chem. Phys*., 10 (2008) 5953–5956.

[33] M. Nedic´, T. N. Wassermann, R. W. Larsen, M. A. Suhm, *Phys. Chem. Chem. Phys*., 13 (2011) 14050–14063.

[34] I. A. Finneran, P. B. Carroll, M. A. Allodi, G. A. Blake, *Phys. Chem. Chem. Phys*. 17 (2015) 24210–24214.

[35] J. Andersen, J. Heimdal, R. Wugt Larsen, *J. Chem. Phys*. 143 (2015) 224315.

[36] B. M. Giuliano, L. B. Favero, A. Maris, W. Caminati, . *Chem. Eur. J.* 18 (2012), 12759-12763.

[37] L. Evangelisti, G. Feng, R. Rizzato, W. Caminati, *ChemPhysChem*, 12 (2011) 1916 -1920.

[38] N. Borho, Y. Xu, *Phys. Chem. Chem. Phys*. 9 (2007) 4514–4520.

[39] N. Borho, Y. Xu, *Angew. Chem. Int. Ed*. 46 (2007) 2276 –2279.

[40] K. S. Buckton, R. G. Azrak, *J. Chem. Phys.* 52 (1970) 5652–5655;
D. Green, S. Hammond, J. Keske, B. H. Pate, *J. Chem. Phys.* 110 (1999) 1979–1989;
D. A. McWhorter, E. Hudspeth, B. H. Pate, *J. Chem. Phys.* 110 (1999) 2000–2009;
C. L. Brummel, S. W. Mork, L. A. Philips, *J. Chem. Phys.* 95 (1991) 7041–7053.

[41] L. H. Xu, G. T. Fraser, F. J. Lovas, R. D. Suenram, C. W. Gillies, H. E. Warner, J. Z. Gillies, *J. Chem. Phys.* 103 (1995) 9541−9548;
J. Marco, J. M. Orza, *J. Mol. Struct.* 267 (1992) 33−38.

Table 1. Predicted spectroscopic parameters for the six lowest-energy conformers of ethanol dimer from *ab initio* computations.[a]

	g+t	***g-t***	***g+g+***	***tt***	***g-g+***	***tg+***
A[b] (MHz)	4824.8	5055.0	5182.5	6312.9	6222.4	6922.5
B (MHz)	1424.0	1361.7	1350.5	1169.7	1216.4	1074.6
C (MHz)	1303.0	1281.3	1266.7	1065.3	1101.0	994.8
μ_a /μ_b /μ_c[c] (D)	2.4/0.1/1.6	2.6/1.2/1.2	2.2/1.5/0.2	2.8/0.1/0.9	2.1/1.5/0.2	2.3/0.9/0.1
ΔE_{MP2}[d] (cm^{-1})	0	6	12	39	92	121
$\Delta E_{MP2+ZPC}$[e] (cm^{-1})	35	5	29	0	80	50
D_e[f] (kJ mol^{-1})	22.17	22.43	23.26	21.76	22.80	22.43

[a] Optimised structures at the MP2/6-311++G(d,p) level of theory
[b] A, B and C are the rotational constants.
[c] μ_a, μ_b, and μ_c are the absolute values of the electric dipole moment components along the principal inertial axes.
[d] Relative electronic energies.
[e] Relative electronic energies including the zero-point correction.
[f] Equilibrium dissociation energies including corrections for the basis set superposition error (see text).

Table 2. Experimental spectroscopic parameters for the three conformers of ethanol dimer *g+g+*, *g+t* and *g–t*.

	g+g+		***g-t***		***g+t***	
	a	**b**	**a**	**b**	**a**	**b**
A[c] / MHz	5113.7747(14)[d]	5113.82340(56)	5086.3946(22)	5086.4568(19)	4851.5896(14)	4851.6034(16)
B / MHz	1329.72053(58)	1329.721221(47)	1316.64918(84)	1316.65057(25)	1369.75568(49)	1369.75623(20)
C/ MHz	1257.51597(43)	1257.515218(43)	1243.63191(82)	1243.63300(25)	1243.41865(64)	1243.41829(16)
D_J / kHz	2.845(24)	2.85516(33)	2.943(37)	2.9772(60)	2.145(24)	2.1211(15)
D_{JK} / kHz	-7.292(81)	-7.4358(36)	-7.569(68)	-7.538(12)	2.830(77)	2.792(18)
D_K / kHz	-	51.07(11)	-	60.08(40)	-	6.97(32)
d_1 / kHz	0.06197(41)	0.05164(20)	0.2056(23)	0.2027(13)	-0.1585(57)	-0.1674(14)
d_2 / kHz	-	-0.04650(20)	-	-0.03162(72)	-	-0.09715(85)
H_J / Hz	-	-	-	0.182(60)	-	-
H_{KJ} / Hz	-	-3.47(15)	-	-4.82(53)	-	-
***a* /*b* /*c*[e]**	y/y/n	y/y/n	y/y/y	y/y/y	y/n/y	y/n/y
σ[f] / kHz	2.8	0.8	6.1	3.5	2.5	5.0
N[g]	23	56	31	69	17	36

[a] Fit including transitions measured in this work.
[b] Global fit including transitions from reference 8.
[c] A, B and C are the rotational constants; D_J, D_{JK}, D_K, d_1, d_2, H_J and H_{KJ} are the centrifugal distortion constants.
[d] Standard error in parentheses in units of the last digit.
[e] Yes (y) or no (n) observation of *a*-, *b*- and *c*-type transitions.
[f] rms deviation of the fit.
[g] Number of fitted transitions.

Table 3. Experimental spectroscopic parameters for the three new observed conformers of ethanol dimer.

	I/ *tt*	**II/ *g-g+***	**III/ *tg+***
A[a] / MHz	6456.6562(14)	6224.8(57)	6876.3(30)
B / MHz	1134.20787(27)	1200.9718(21)	1071.89890(52)
C/ MHz	1034.40552(26)	1090.7944(21)	985.79204(52)
D_J / kHz	1.5437(56)	3.50(12)	1.633(29)
D_{JK} / kHz	-6.267(34)	-28.99(51)	-15.71(12)
d_1 / kHz	-0.21670(89)	-	-
***a* /*b* /*c* [c]**	y/n/y	y/n/n	y/n/n
σ [d] (kHz)	2.8	6.7	1.7
N [e]	25	9	9

[a] A, B and C are the rotational constants; D_J, D_{JK} and d_1 are the centrifugal distortion constants.
[b] Standard error in parentheses in units of the last digit.
[c] Yes (y) or no (n) observation of *a*-, *b*- and *c*-type transitions.
[d] rms deviation of the fit.
[d] Number of fitted transitions.

Table 4. Experimental spectroscopic constants for the ^{13}C isotopologues of conformer *tt*.

	$^{13}C_1$	**$^{13}C_2$**	**$^{13}C_5$**	**$^{13}C_6$**	**$^{18}O_3$**	**$^{18}O_4$**
A[a] / MHz	6442.7(53) [b]	6437.2(14)	6455.8(32)	6316.4(53)	6356.2(54)	6310.9(36)
B / MHz	1108.5885(15)	1125.12353(42)	1118.12206(55)	1125.1213(18)	1126.8410(11)	1121.1609(14)
C/ MHz	1012.7422(15)	1027.30633(42)	1021.08439(55)	1023.0783(18)	1028.63479(93)	1019.8736(13)
D_J/ kHz	[1.5437]	[1.5437]	[1.5437][e]	[1.5437]	[1.5437]	[1.5437]
D_{JK}/ kHz	[-6.267]	[-6.267]	[-6.267]	[-6.267]	[-6.267]	[-6.267]
d_1 / kHz	[-0.21670]	[-0.21670]	[-0.21670]	[-0.21670]	[-0.21670]	[-0.21670]
σ [c] / KHz	7.3	2.0	2.5	8.6	4.1	5.8
N [d]	8	8	6	8	5	6

[a] A, B and C are the rotational constants.
[b] Standard error in parentheses in units of the last digit.
[c] rms deviation of the fit.
[d] Number of fitted transitions.
[e]The centrifugal distortion constants in square brackets have been kept fixed to the value of the parent species.

Table 5. Experimental spectroscopic constants for the ^{13}C isotopologues of conformer *g+g+*.

	$^{13}C_1$	$^{13}C_2$	$^{13}C_5$	$^{13}C_6$
A[a] / MHz	5047.3(32)[b]	5107.3(46)	5097.7(41)	5072.9(53)
B / MHz	1311.51477(60)	1311.6655(14)	1317.2897(13)	1308.69944(95)
C/ MHz	1240.02043(60)	1241.1220(14)	1245.5145(13)	1237.99507(95)
D_J/ kHz	[2.845]	[2.845]	[2.845]	[2.845][e]
D_{JK}/ kHz	[-7.292]	[-7.292]	[-7.292]	[-7.292]
d_1 / kHz	[0.06197]	[0.06197]	[0.06197]	[0.06197]
σ[c] / KHz	2.7	6.8	6.2	4.2
N[d]	6	8	8	6

[a] A, B and C are the rotational constants.
[b] Standard error in parentheses in units of the last digit.
[c] rms deviation of the fit.
[d] Number of fitted transitions.
[e]The centrifugal distortion constants in square brackets have been kept fixed to the value of the parent species.

Table 6. Experimental spectroscopic constants for the ^{13}C isotopologues of conformer *g–t*.

	$^{13}C_1$	$^{13}C_2$	$^{13}C_5$	$^{13}C_6$
A[a] / MHz	5044.2(49)[b]	5072.7(24)	5082.1(26)	5016.2(11)
B / MHz	1294.0766(21)	1303.98009(45)	1297.85605(79)	1302.40509(39)
C/ MHz	1224.0078(18)	1231.20182(45)	1226.73292(79)	1228.19380(39)
D_J/ kHz	[2.943]	[2.943]	[2.943][e]	[2.943]
D_{JK}/ kHz	[-7.569]	[-7.569]	[-7.569]	[-7.569]
d_1 / kHz	[0.2056]	[0.2056]	[0.2056]	[0.2056]
σ[c] / KHz	7.3	2.0	3.8	1.8
N[d]	7	6	8	7

[a] A, B and C are the rotational constants.
[b] Standard error in parentheses in units of the last digit.
[c] rms deviation of the fit.
[d] Number of fitted transitions.
[e]The centrifugal distortion constants in square brackets have been kept fixed to the value of the parent species.

Table 7. Carbon and oxygen substitution coordinates of conformer *tt* in angstroms.

	Experiment			Ab initio[c]		
	$\|a\|$	$\|b\|$	$\|c\|$	*a*	*b*	*c*
C_1	3.2190(51)[a]	0.409(41)	0.09(18)	-3.165	0.438	-0.026
C_2	1.8417(25)	0.087(52)	0.4823(95)	-1.842	-0.094	0.492
O_3	1.0594(82)	0.518(17)	0.605(15)	-1.067	-0.511	0.622
O_4	1.6194(37)	0.9623(63)	0.092(69)	1.587	-0.991	0.327
C_5	2.5367(39)	[0][b]	0.155(65)	2.488	-0.010	-0.211
C_6	1.9092(88)	1.344(13)	[0][b]	1.888	1.357	0.052

[a]Derived errors in parentheses in units of the last digit. These were calculated according to Constain's formula: $\sigma(x)=K/|x|$; $\sigma(x)$ is the error in the coordinate x and K=0.0012 Å
[b] Value constrained to zero.
[c] MP2/6-311G++(d,p) level of theory

Table 8. Carbon substitution coordinates of conformer *g*+*g*+ in angstroms.

	Experiment			Ab initio[b]		
	$\|a\|$	$\|b\|$	$\|c\|$	*a*	*b*	*c*
C_1	2.1992(73)[a]	0.92247	0.694(24)	2.177	-0.940	-0.615
C_2	2.2900(98)	0.32195	0.16(14)	2.281	0.354	0.182
C_5	1.896(10)	0.552(37)	0.12(18)	-1.860	-0.634	-0.266
C_6	2.419(10)	0.722(37)	0.544(50)	-2.481	0.715	-0.586

[a]Derived errors in parentheses in units of the last digit. These were calculated according to Constain's formula: $\sigma(x)=K/|x|$; $\sigma(x)$ is the error in the coordinate x and K=0.0012 Å
[b] MP2/6-311G++(d,p) level of theory

Table 9. Carbon substitution coordinates of conformer *g*–*t* in angstroms.

	Experiment			Ab initio[c]		
	$\|a\|$	$\|b\|$	$\|c\|$	*a*	*b*	*c*
C_1	2.4938(98)[a]	0.572(43)	0.726(35)	2.442	-0.648	-0.714
C_2	1.9511(61)	0.573(21)	[0][b]	1.932	0.647	-0.096
C_5	2.3614(54)	0.252(52)	0.150(88)	-2.327	-0.256	0.112
C_6	1.9921(29)	1.0782(54)	0.507(12)	-1.992	1.048	-0.583

[a]Derived errors in parentheses in units of the last digit. These were calculated according to Constain's formula: $\sigma(x)=K/|x|$; $\sigma(x)$ is the error in the coordinate x and K=0.0012 Å
[b] Value constrained to zero.
[c] MP2/6-311G++(d,p) level of theory

Table 10. Comparison of the bond lengths (in Å) and angles (in degrees) of conformer *tt* determined experimentally and theoretically.

	r_s	r_0	MP2/ 6-311++G(d,p)	MP2/ 6-311++G(3df,2p)	M062X/ 6-311++G(d,p)	M062X/ 6-311++G(3df,2p)
$r(C_1–C_2)$	1.572(71)[a]	1.521(35)	1.517	1.512	1.515	1.514
$r(O_3–C_2)$	1.407(22)	1.351(28)	1.421	1.417	1.415	1.411
$r(O_3–O_4)$	2.803(20)	2.889(22)	2.859	2.853	2.843	2.863
$r(O_4–C_5)$	1.352(64)	1.479(32)	1.437	1.432	1.430	1.426
$r(C_5–C_6)$	1.492(80)	1.492(42)	1.516	1.510	1.514	1.512
$\angle O_3–C_2–C_1$	107.6(63)	116.0(41)	108.1	108.0	108.2	108.4
$\angle O_4–O_3–C_2$	112.8(15)	110.32(81)	107.2	107.7	103.4	103.4
$\angle O_4–C_5–C_6$	109.7(19)	105.9(11)	107.6	107.4	107.7	107.9
$\angle O_4–O_3–C_2–C_1$	168.3(23)	-	168.5	172.1	160.6	159.6
$\angle C_2–O_3–O_4–C_5$	-97.9(56)	-112.5(31)	-111.9	-108.5	-105.8	-107.4
$\angle C_5–C_6–C_2–C_1$	-138.3(83)	-	-137.5	-133.1	-146.9	-145.8

[a]Derived errors in parentheses in units of the last digit

Table 11. Comparison of the bond lengths (in Å) and angles (in degrees) of conformer *g+g+* determined experimentally and theoretically.

	r_s	MP2/ 6-311++G(d,p)	MP2/ 6-311++G(3df,2p)	M062X/ 6-311++G(d,p)	M062X/ 6-311++G(3df,2p)
$r(C_2–C_1)$	1.51(10) [a]	1.523	1.518	1.522	1.520
$r(C_5–C_6)$	1.443(72)	1.520	1.514	1.518	1.516
$\tau C_5–C_6–C_2–C_1$	-49.3(89)	-39.7	-41.7	-33.0	-32.1

[a]Derived errors in parentheses in units of the last digit

Table 12. Comparison of the bond lengths (in Å) and angles (in degrees) of conformer *g–t* determined experimentally and theoretically.

	r_s	MP2/ 6-311++G(d,p)	MP2/ 6-311++G(3df,2p)	M062X/ 6-311++G(d,p)	M062X/ 6-311++G(3df,2p)
$r(C_2–C_1)$	1.461(49)[a]	1.523	1.518	1.521	1.519
$r(C_5–C_6)$	1.529(59)	1.515	1.510	1.514	1.512
$\tau C_5–C_6–C_2–C_1$	63.5(41)	57.4	59.5	61.9	63.7

[a]Derived errors in parentheses in units of the last digit

Figure 1. The three conformations of ethanol.

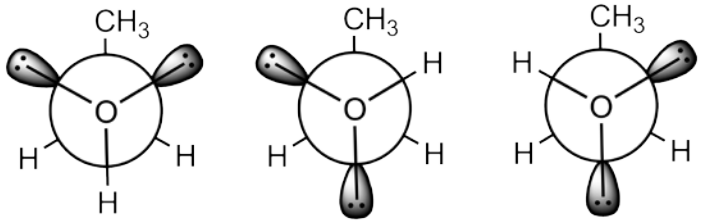

Figure 2. Broadband rotational spectra of ethanol dimer collected using Helium (1033k FIDs), Neon (1250k FIDs) and Argon (1162k FIDs) as carrier gases in the 2-8 GHz frequency range. The upper trace shows the experimental rotational spectrum while the lower trace shows the rotational spectrum simulated using the experimental rotational constants.

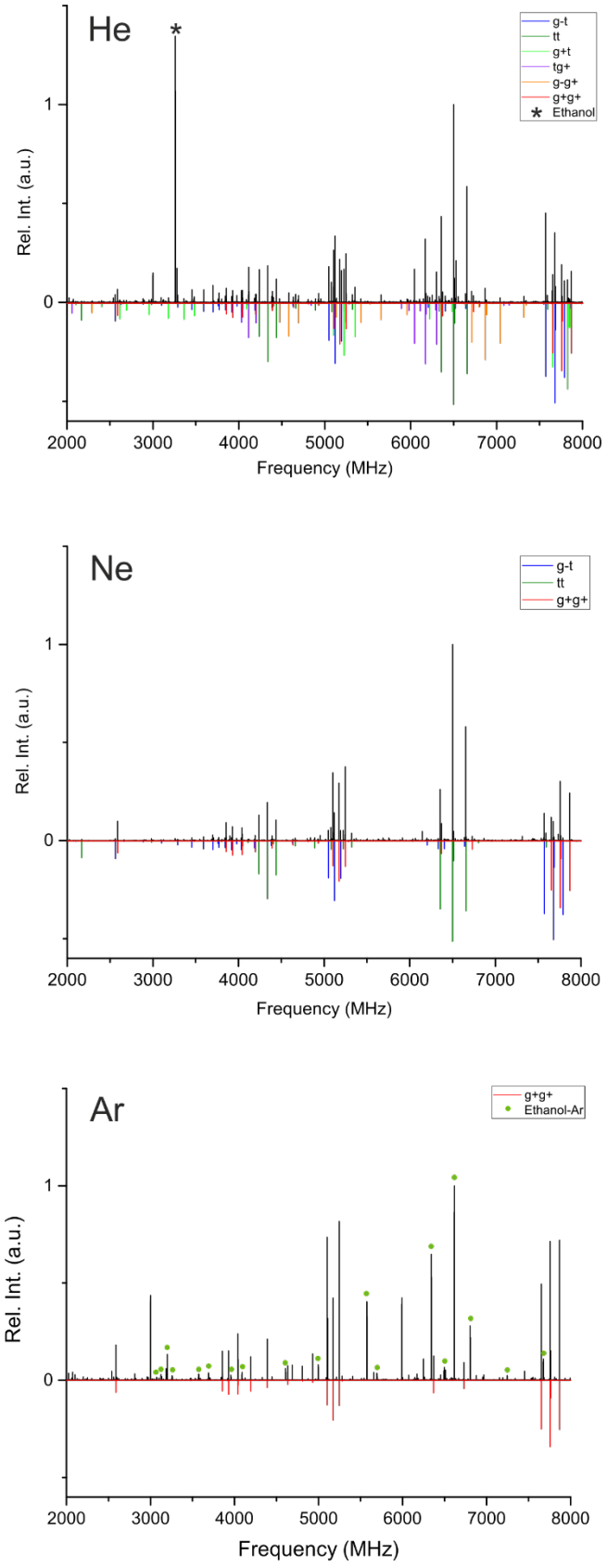

Figure 3. Scheme of the molecular structure of ethanol dimer showing the numbering of the heavy atoms.

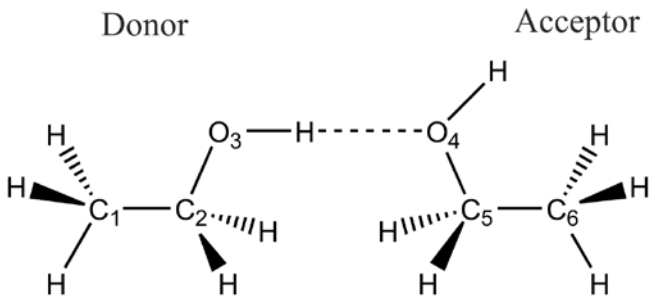

Figure 4. The six observed conformers of ethanol dimer showing the intermolecular hydrogen bond interactions according to MP2/6-311G++(d,p) structures.